energies

MDPI

Article

Effect of Volcanic Events on Hydrocarbon Generation of Lacustrine Organic-Rich Shale: An Example of the Upper Triassic Galedesi Formation in the Hala Lake Depression, South Qilian Basin, China

Jia Wang [1,*], Chaobin Zhu [1], Xianfeng Tan [1,*], Long Luo [1], Nan Jiang [1], Xuejiao Qu [1], Xuanbo Gao [1], Shengyu Li [1], Long Xiao [2] and Haijun Liu [3]

[1] Chongqing Key Laboratory of Complex Oil and Gas Exploration and Development, Chongqing University of Science & Technology, Chongqing 401331, China; zhuchaobin2022@163.com (C.Z.); longluo988@163.com (L.L.); dou_508@163.com (N.J.); quxuejiao2008@aliyun.com (X.Q.); gaoxuanbo@cqust.edu.cn (X.G.); 2021005@cqust.edu.cn (S.L.)
[2] Qinghai Coal Geological Exploration Institute, Xining 810008, China; qhmkxl@163.com
[3] China Southwest Geotechnical Investigation & Design Institute Co., Ltd., Chengdu 610052, China; lhjjc8@163.com
* Correspondence: wangjia@cqust.edu.cn (J.W.); xianfengtan8299@163.com (X.T.)

Abstract: The thermal evolution process of organic matter is associated with the complete hydrocarbon generation and expulsion process in shale, however, the thermal evolution of organic matter is a long process and cannot be realized without experimental simulations. Although several scholars have substantially studied the thermal evolution of organic matter, it remains a challenging and much debated issue in the studies of organic geochemistry. Volcanic events are crucial in the enrichment of organic matter, and appropriate heating accelerates the thermal evolution of organic matter. However, how strong-rock baking restricts the evolution of organic matter in shale has not been specifically studied. The South Qilian Basin in China is a typical superimposed basin where complex tectonic movements have induced multiple volcanic events, which makes it a favorable location to perform the aforementioned research. This study used the Galedesi Formation shale in the Hala Lake Depression of the South Qilian Basin as an example for investigating the constraints of the volcanic events related to the thermal evolution of organic matter by integrating the results obtained using the geochemical and petrological methods. Our results demonstrate that the lacustrine Galedesi Formation shale of the Hala Lake Depression in the Late Triassic is a typical deep-lake facies deposit with good hydrocarbon generation potential. However, because of the influence of regional tectonic evolution, the burial depth of shale is not deep and the thermal evolution of organic matter is insufficient. Due to the influence of multiple volcanic thermal events in the later stages, the thermal maturity of organic matter in the Galedesi Formation shale generally exceeds 3.0%, which is abnormally high. The apparent carbonization of organic matter can be observed via scanning electron microscopy. Rapid magma baking typically cannot effectively promote the hydrocarbon generation of shale organic matter. Finally, the burial depth of lacustrine shale of the Galedesi Formation in the Hala Lake Depression of South Qilian Basin is too shallow. Organic matter hydrocarbon generation and later shale preservation conditions are not conducive to the enrichment, accumulation, exploration, and development of shale gas.

Keywords: organic matter; thermal evolution; shale; Galedesi Formation; South Qilian Basin

Citation: Wang, J.; Zhu, C.; Tan, X.; Luo, L.; Jiang, N.; Qu, X.; Gao, X.; Li, S.; Xiao, L.; Liu, H. Effect of Volcanic Events on Hydrocarbon Generation of Lacustrine Organic-Rich Shale: An Example of the Upper Triassic Galedesi Formation in the Hala Lake Depression, South Qilian Basin, China. *Energies* **2022**, *15*, 3818. https://doi.org/10.3390/en15103818

Academic Editors: Xixin Wang and Reza Rezaee

Received: 20 February 2022
Accepted: 13 May 2022
Published: 22 May 2022

1. Introduction

With the advancement of shale oil and gas exploration and development, research on the hydrocarbon generation potential and processes of organic shale has attracted increasing attention [1–5]. Several factors affect the hydrocarbon generation processes

of various organic matter such as the burial history, temperature, pressure, and fluid properties. The hydrocarbon generation capacity of organic matter correlates with the degree of the oil and gas enrichment in shale [6,7]. However, the current research on the influence of abnormal thermal events on organic matter hydrocarbon generation is inadequate, and whether the various thermal events are constructive or destructive in organic matter hydrocarbon generation remain unclear. This limits the advancement of shale oil and gas exploration as well as development in the areas with strong compressive tectonic background.

Volcanic thermal events studies have focused on metal deposits, event deposition, hydrothermal activity, alteration mineralogy, and petrophysics [8–10]. Volcanic hydrothermal fluids can promote metal-rich mineral crystallization in the compressive fault structural belt to form hydrothermal deposits. Volcanic ash can be deposited to form a thin tuffaceous sedimentary layer, providing nutrients for seabed organisms, promoting plankton reproduction, and increasing marine paleoproductivity [11–13].

As a tectonic-superimposed basin with a typical compressional tectonic background and frequent volcanic thermal events, the South Qilian Basin in China is a potential enrichment zone for metal deposits [14,15]. Lacustrine organic-matter-rich shale developed in the South Qilian Basin, which is an ideal location for studying the thermal evolution mechanisms of organic matter caused by abnormal thermal events. Therefore, considering the shale of the Upper Triassic Galedesi Formation in the Hala Lake Depression of the South Qilian Basin as an example, this study investigates the relationship between the volcanic thermal events and hydrocarbon generation processes of lacustrine organic-matter-rich shale to provide new theoretical support for the investigation of the thermal evolution of terrestrial shale organic matter.

2. Geological Setting

The South Qilian Basin in the northeastern Qinghai Tibet Plateau is a typical superimposed basin in western China [16,17] (Figure 1). The Hala Lake Depression is in the northwestern South Qilian Basin. Since the Caledonian orogeny, multi-stage structures have transformed the Hala Lake Depression into a typical fault depression, and the strata of the Atasi Formation and Galedesi Formation are exposed on the surface.

Since the Middle Permian, the sedimentary environment of the Hala Lake area has primarily comprised shallow sea facies. Following the Hercynian orogeny, the marine–continental transition occurred, the marine–continental transition facies deposition began, and many marine–continental deposits were developed. More than 1000 m of lacustrine clastic rocks were deposited until the Late Triassic. After the Late Triassic, the Indosinian orogeny uplifted the Hala Lake area on a large-scale and the lake became a typical denudation area in the South Qilian region, lacking the Jurassic and Cretaceous outcrops in the study area. In the Himalayan period of the Cretaceous, affected by the long-range effect of the subduction and collision of the Indian plate to the Eurasian plate, the depression became an uplift fold belt and developed a series of thrust faults [18,19]. The tectonic line in the study area primarily trends northwest to southeast, and the folds as well as the faults developed due to collision orogeny (Figure 1).

The basement at the Hala Lake Depression comprises the Silurian metamorphic, which unconformably contacts the overlying sedimentary strata (Figure 2). The basement Silurian sericite schist developed in the uplift area. The Permian, Triassic, and the younger strata are widely distributed in the depression area.

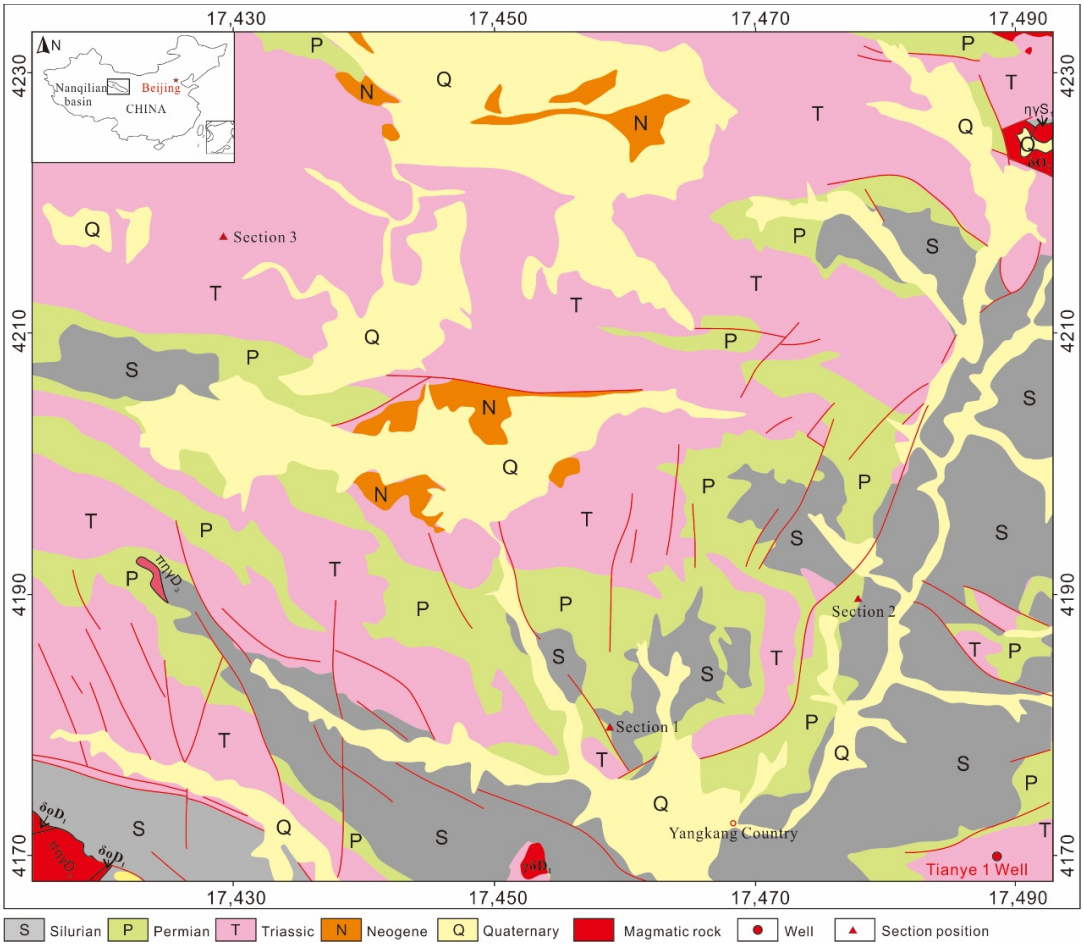

Figure 1. The regional structural characteristics of the study area.

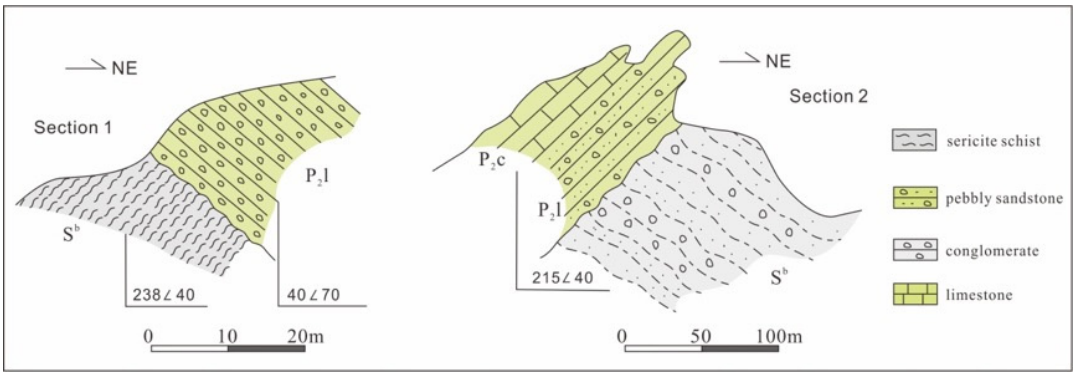

Figure 2. Schematic diagram of the structural and stratigraphic in sections (section locations are shown in Figure 1).

3. Samples and Methods

A total of 113 shale samples were collected from the two sections of the Galedesi Formation in the Hala Lake Depression and analyzed via organic geochemistry data, the inclusion temperature measurement method, and scanning electron microscopy. All samples were analyzed and tested at the State Key Laboratory of Oil and Gas Reservoir Geology and Exploitation, Chengdu University of Technology and the Sichuan Coalfield Geology Bureau. The homogenization temperatures of the 19 fluid inclusions found in the shale veins and cements were measured by the Linkam cold and hot platform (THMSG

600, Linkam, UK). Before the tests, the inclusion sheets were polished and soaked using an intelligent sheet automatic polishing machine (ZMP-1000ZS, Tianjing, China).

All debris samples (diameter less than 1 cm) were selected and dried at a low temperature before being ground into a 200-mesh. To remove the carbonate minerals before testing, 10% hydrochloric acid was added to each sample in a centrifuge tube and a glass beaker. The total organic carbon (TOC) content and bitumen reflectance (Rb) of all the shale samples were analyzed using a LECO CS230 (Leco, St. Joseph, MO, USA) carbon and a Leica MPV-III (Leica, Weztlar, Germany) microphotometer under oil immersion, respectively. Moreover, the temperatures at the maximum hydrocarbon generation (Tmax) were determined using ROCK-EVAL 6 (Vinci, Paris, France) at the Sichuan Coalfield Geology Bureau.

All microscopic analyses (scanning electron microscopy and the nitrogen adsorption experiment) were conducted at the State Key Laboratory of Oil and Gas Reservoir Geology and Exploitation, Chengdu University of Technology, China. A Quanta FEG 250 (FEI, Hillsboro, OR, USA) environmental field emission scanning electron microscope was used with image magnifications from 10 to 500,000.

4. Results

4.1. Sedimentary Evolution Characteristics

The shale in the study area is a typical deep lacustrine black shale, which is rich in more terrigenous input minerals and is remarkably different from the current marine shale sedimentary environments compared to North America and southern China [15,20]. During the shale deposition period of the Galedesi Formation in the Late Triassic in the Hala Lake Depression, continental lacustrine facies and a sedimentary environment with distinct biomarkers can be identified (Figure 3) [21]. The Shulenanshan Mountain in the north and Yangkang Uplift in the south provided sediment sources for the Hala Lake Depression in the Late Triassic. A large set of black organic-rich shale was deposited in the Hala Lake Depression, and alluvial fan as well as fan delta facies and clastic deposits were developed at the edge of the lake basin [19].

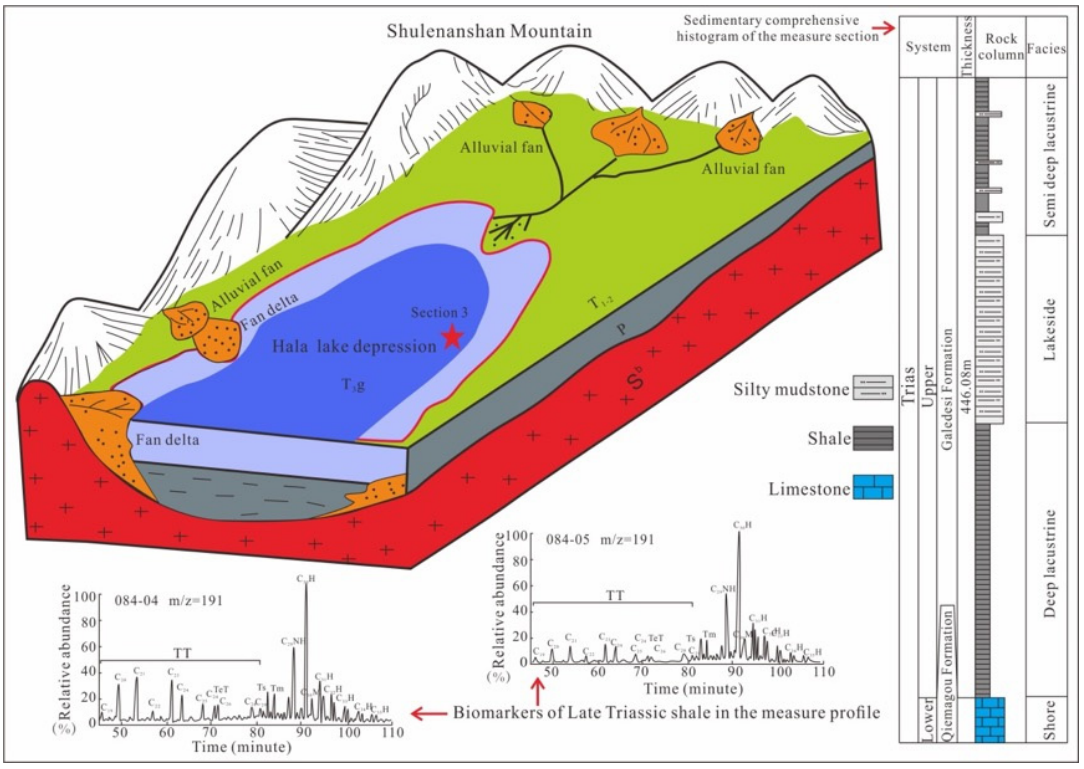

Figure 3. The sedimentary facies model of the Galedesi Formation shale in the Hala Lake Depression (Section 3 locations are shown in Figure 1).

In addition to the regional evolutionary events, the entire Hala Lake Depression was strongly affected by the Indosinian orogeny, resulting in the early intra-continental lake basin rising to an intra-continental highland that underwent weathering as well as denudation. Therefore, the shale of the Galedesi Formation in the Hala Lake Depression area is not completely preserved. As part of an argillaceous siltstone in the upper part of the Galedesi Formation is denuded, the Jurassic and subsequent strata are missing.

4.2. Organic Geochemical Characteristics

The data obtained from the organic geochemical analysis and testing of 113 lacustrine black shale samples collected from the Galedesi Formation exhibited strong hydrocarbon generation potential after undergoing high thermal evolution (Table 1, Figure 4).

Table 1. Shale organic geochemical analysis data.

Test Type	Number of Samples	Minimum	Maximum	Average	Result
TOC (%)	113	0.47	2.68	1.62	Good level
Ro (%)	66	2.82	4.13	3.65	Over mature
$\delta^{13}C$ (%)	113	−28.89	−24.83	−26.90	II_2 kerogen
H/C	66	0.07	0.62	0.28	III kerogen
O/C	66	0.02	0.36	0.19	

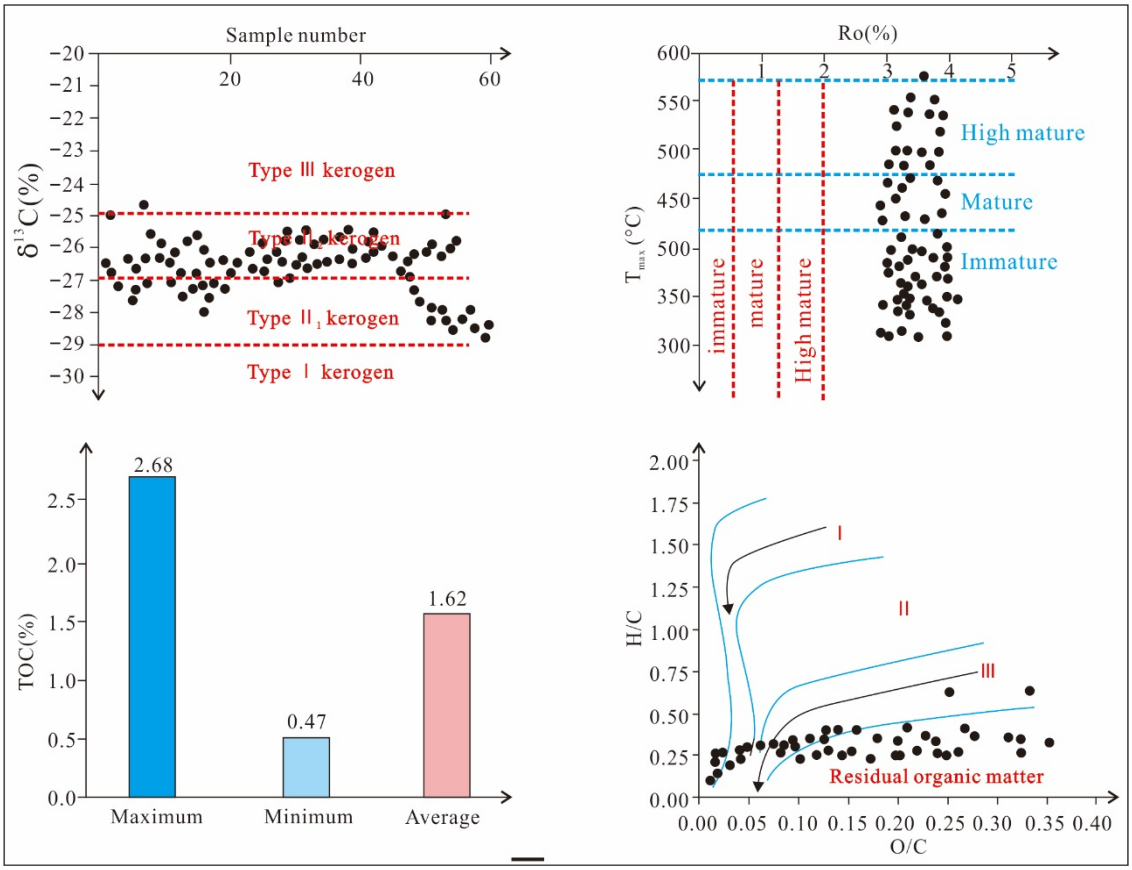

Figure 4. Organic geochemical parameters of the Galedesi Formation shale.

First, the average value of the total organic carbon (TOC) was as high as 1.62, indicating good hydrocarbon generation potential, and the vitrinite reflectance generally exceeded 3.0% (average = 3.65%), which was much higher than that of the marine shale in southern China. Based on the organic matter isotope ($\delta^{13}C$) analysis and the elemental ratio (H/C

and O/C), the types of kerogen in shale were inconsistent, which may be attributed to the abnormally high thermal evolution process (R_o > 2.0%). The analysis of the H/C and O/C data is unreliable, and the possibility of the occurrence of type-II_2 kerogen is greater.

In addition, the TOC value, total hydrocarbon, and field analytical gas content of the Galedesi Formation shale at different depths in the Tianye 1 Well were measured (Table 2). The TOC value was between 0.04% and 5.61% (average = 1.26%). The total hydrocarbon value was 0.0003~0.306% (average = 0.099%). The field analytical data showed that most of the shale did not contain natural gas (maximum content = 0.115 m^3/t). Scanning electron microscopy showed that a large amount of carbonated organic matter is present in the Galedesi Formation shale (Figure 5).

Table 2. The field analysis data of the Galedesi Formation shale in the Tianye 1 Well.

Sample Number	Well Depth (m)	TOC (%)	Total Hydrocarbon (%)	Gas Content (m^3/t)
1	20.62	2.90	/	/
2	67.74	1.77	/	/
3	123.15	1.10	0.0876	0.0600
4	171.36	1.00	0.3062	0.1150
5	196.46	1.28	0.0824	/
6	255.67	0.73	0.0584	/
7	272.90	1.11	0.1840	/
8	299.40	1.52	0.1726	/
9	356.05	2.13	0.2537	/
10	385.50	0.25	0.0501	/
11	395.20	2.06	0.0965	/
12	418.50	2.84	0.0939	/
13	451.05	1.75	0.0524	/
14	468.30	3.06	0.1321	/
15	500.70	5.61	0.0801	/
16	516.70	0.74	0.1822	/
17	527.00	0.47	0.1179	0.0100
18	607.60	0.33	0.1225	/
19	627.04	0.20	0.0430	/
20	655.80	0.21	0.0412	/
21	664.60	0.35	0.1696	/
22	675.00	0.04	0.1036	/
23	692.60	0.13	0.1216	/
24	717.60	1.78	0.1468	/
25	744.34	1.40	0.1440	/
26	783.28	0.04	0.0776	/
27	816.00	1.20	0.0635	0.0500
28	852.60	0.97	0.1237	/
29	866.60	1.12	0.0373	/
30	887.90	0.93	0.0918	/
31	921.90	1.10	0.0580	0.0800
32	1067.90	1.37	0.0052	0.0500
33	1088.64	1.02	0.0036	0.0200
34	1105.45	0.74	0.0698	0.0400
35	1148.70	2.54	0.0074	0.0300
36	1156.18	1.50	0.0063	/
37	1168.50	2.94	0.0700	0.0600
38	1303.50	0.15	0.0063	0.0500
39	1321.90	0.45	0.0004	0.0500
40	1338.90	0.72	0.0003	0.0500
41	1362.10	0.75	0.2576	0.0400
42	1420.60	0.67	0.0729	0.0700
43	1443.30	1.05	0.2161	0.0500
44	1478.40	1.33	0.1811	0.0500

Remarks: "/" indicates that the value was lower than the detection range of the instrument.

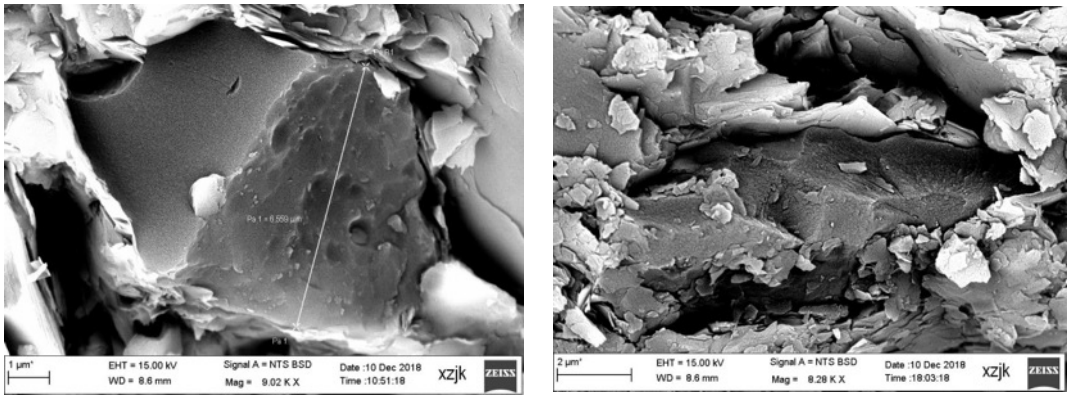

(a) **(b)**

Figure 5. Microscopic characteristics of the carbonized organic matter in shale. (**a**) Tianye 1 Well, 1148.70 m, organic matter. (**b**) Section 1, Organic matter.

4.3. Diagenetic Fluid Properties

A total of 19 hydrocarbon and liquid inclusions were found in the veins and calcite cements of the Galedesi Formation shale. Under the microscope (Leica MPV-III), the hydrocarbon inclusions were blue (Figure 6), and the homogenization temperature test showed that the formation temperature of the hydrocarbon inclusions was concentrated at 170–180 °C and the diagenetic as well as the cementation temperatures of calcite were at 120–130 °C and 170–180 °C. Oil and gas accumulation mainly corresponded to the cementation and formation of calcite veins in the late tectonic movement (Figure 6). The inclusion temperature showed that the maximum diagenetic temperature of the shale exceeded 200 °C, and the tectonic hydrothermal events were obviously multi-stage.

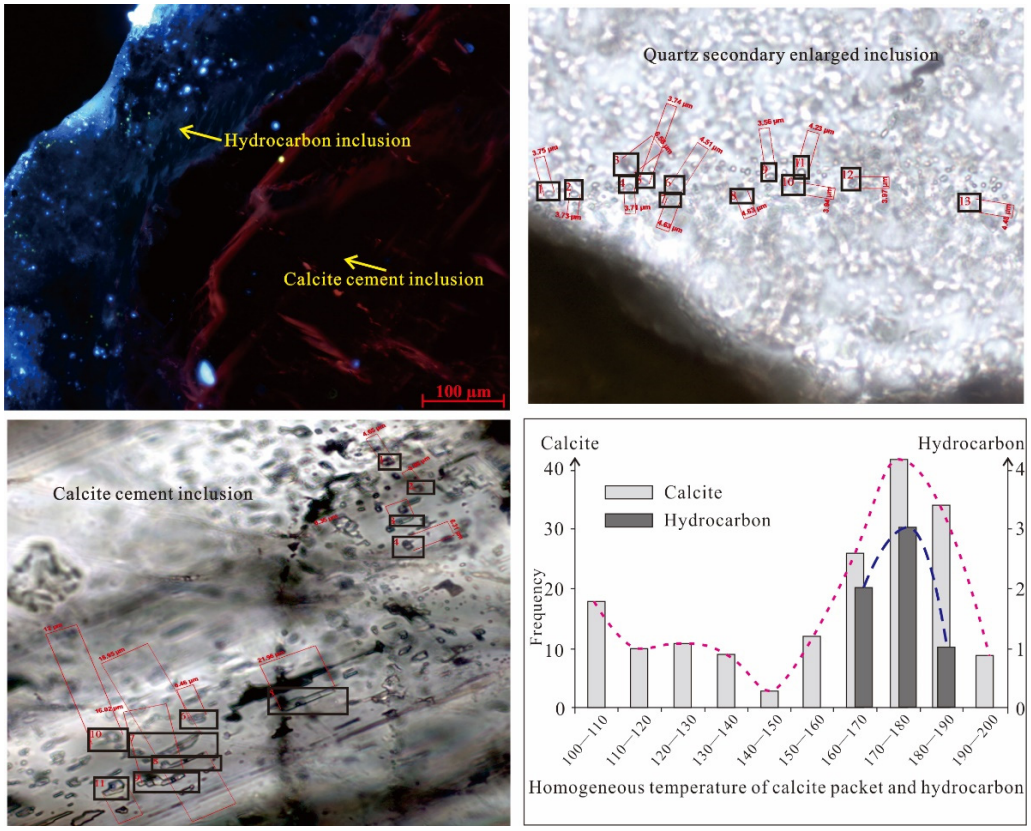

Figure 6. The microscopic characteristics and homogenization temperature range of the fluid inclusions.

4.4. Characteristics of the Reservoir Pore Structure

A total of 21 nitrogen adsorption experiments conducted on the samples collected from the Tianye 1 Well in the Galedesi Formation showed that the adsorption curve mainly indicated the presence of the medium-large pore type (Figure 7). Calculated via the BJH method, the nano-pores of the Galedesi Formation shale in the study area were mainly meso-pores and macro-pores, and the pores measuring less than 10 nm (micro-pore) accounted for only 16.4% (Table 3).

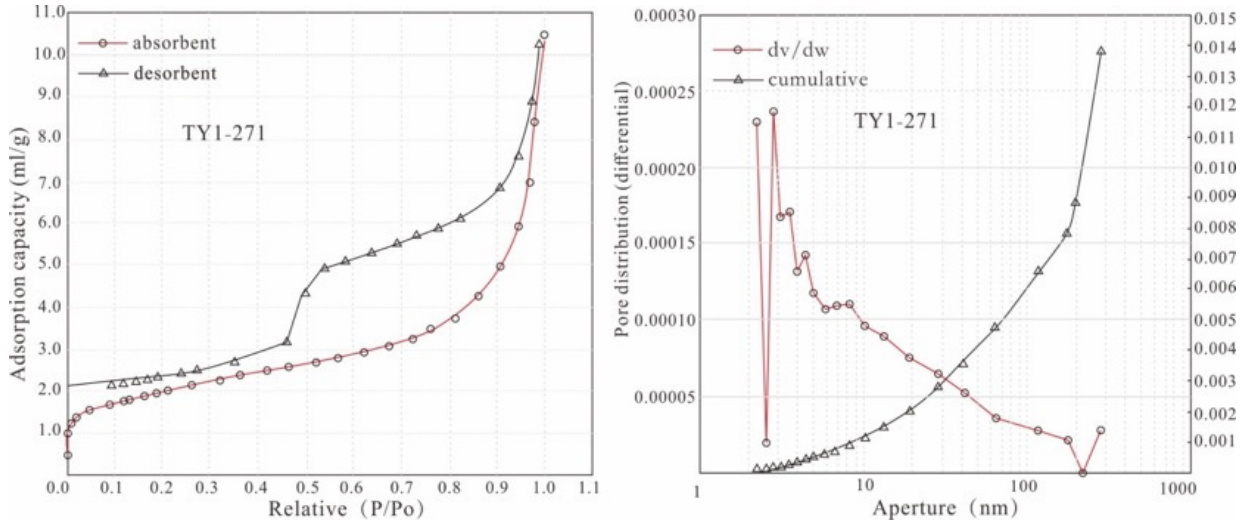

Figure 7. The nitrogen adsorption and desorption curves of the Galedesi Formation shale.

Table 3. Data of the pore volume distribution measured using the nitrogen adsorption method.

Sample Number	Pore Volume (cm^3/g)				Percentage of Pore Volume (%)		
	<10 nm	10~00 nm	>100 nm	Total Pore Volume	<10 nm	10~00 nm	>100 nm
TY1-D01	0.0237	0.0421	0.0283	0.0941	25.19	44.74	30.07
TY1-D02	0.0144	0.0375	0.0695	0.1214	11.86	30.89	57.25
TY1-D03	0.0148	0.041	0.0135	0.0693	21.36	59.16	19.48
TY1-D04	0.0495	0.0595	0.0162	0.1252	39.54	47.52	12.94
TY1-D05	0.012	0.0378	0.0151	0.0694	18.49	58.24	23.27
TY1-D06	0.0117	0.0346	0.0151	0.0614	19.06	56.35	24.59
TY1-D07	0.0187	0.0514	0.0201	0.0902	20.73	56.98	22.28
TY1-D08	0.0103	0.0354	0.0317	0.0774	13.31	45.74	40.96
TY1-D09	0.0128	0.0377	0.0138	0.0643	19.91	58.63	21.46
TY1-D10	0.0071	0.0233	0.0094	0.0398	17.84	58.54	23.62
TY1-D11	0.0052	0.0192	0.0172	0.0416	12.50	46.15	41.35
TY1-D12	0.0044	0.0157	0.0372	0.0573	7.68	27.40	64.92
TY1-D13	0.0088	0.0244	0.0178	0.0510	17.25	47.84	34.90
TY1-D14	0.0098	0.0259	0.0197	0.0554	17.69	46.75	35.56
TY1-D15	0.0103	0.0264	0.051	0.0787	11.74	30.10	58.15
TY1-D16	0.0096	0.0255	0.0459	0.0810	11.85	31.48	56.67
TY1-D17	0.006	0.0218	0.0486	0.0764	7.85	28.53	63.61
TY1-D18	0.0058	0.0229	0.0204	0.0491	11.45	46.83	41.72
TY1-D19	0.0092	0.0092	0.0092	0.0426	20.75	57.55	21.70
TY1-D20	0.0118	0.0274	0.0541	0.0934	12.74	29.34	57.92
TY1-D21	0.0047	0.0167	0.0499	0.0713	6.59	23.42	69.98
Average value	0.0124	0.0303	0.0287	0.0719	16.45	44.39	39.16

5. Discussion

5.1. Evidence and Models of Volcanic Events

The discovery of magmatic rocks on the surface is the most direct evidence to confirm the existence of volcanic events. However, volcanic magmatic eruptions are not always completely ejected from the surface and another type of volcanic event is underground intrusion [22–24]. The burial history map of the Galedesi Formation shale was obtained by the Basin Modeling software (Figure 8), where the burial depth of the Galedesi Formation shale in the Hala Lake Depression should be less than 1500 m, the paleogeothermal temperature should be lower than 65 °C, and the thermal maturity of organic matter should be low maturity or immature. However, the measured homogenization temperature of the inclusions in the study area was as high as 200 °C (Figure 6) and the vitrinite reflectance showed that the thermal evolution of organic matter reached the over-mature stage (Table 1). These findings indicate the occurrence of abnormal volcanic events that accelerated the carbonization process of organic matter, thereby giving the impression of the high-thermal maturity of the organic matter.

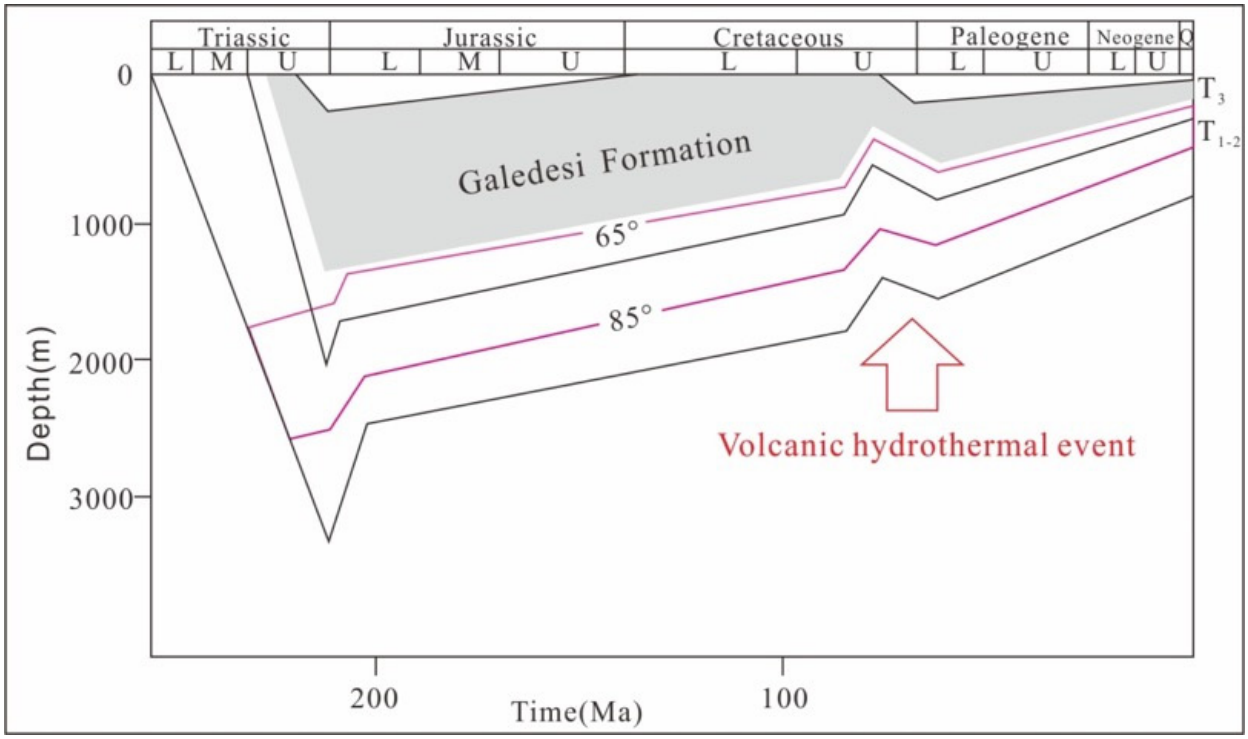

Figure 8. The burial history map of the Galedesi Formation shale in the study area.

Since the Caledonian movement, the entire South Qilian Basin has undergone multi-stage volcanic intrusion and eruption events and many sets of exhalative rock combinations are exposed on the surface [25,26]. However, the post-Triassic magma is mainly exposed on the surface to the south of the study area [27]. During the Indosinian orogeny in the Late Triassic, the volcanic events in the study area were dominated by intrusion and the magma mainly overflowed along the early angular unconformity (Figure 9), which can be attributed to the abundance of solid minerals in the study area.

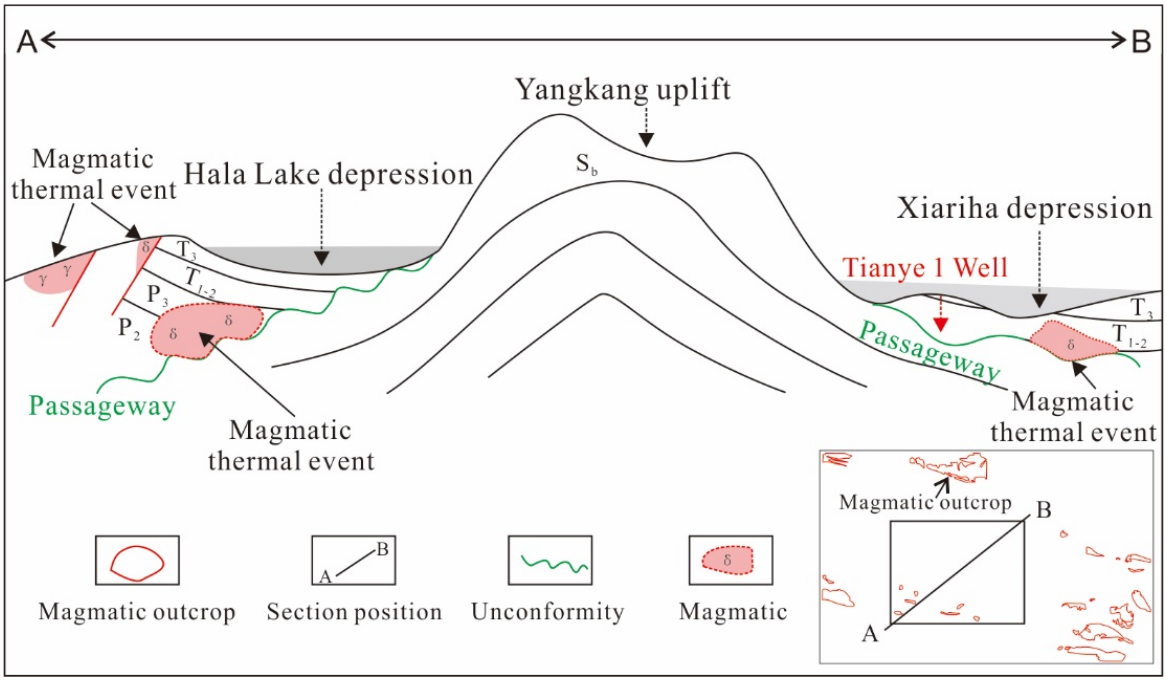

Figure 9. The model map of the magmatic thermal events in the study area.

5.2. Constraints of Volcanic Thermal Events on the Evolution of Shale Organic Matter

With the increasing shale gas exploration and development in recent years, continental organic-rich shale has gradually become the focus of geologists [28–31]. Although the hydrocarbon generation potential of continental shale is generally worse than that of marine shale, continental shale often has a shallower burial depth and good reservoir capacity [32,33].

The test data showed that the Galedesi Formation in the Hala Lake Depression has good organic carbon enrichment capacity; however, the field analysis data obtained from Tianye 1 Well showed that the total hydrocarbon content is generally lower than 0.1% (Table 2), there is almost no shale gas, and the gas content is very low. Therefore, the volcanic thermal events caused the rapid thermal evolution of organic matter in the Galedesi Formation shale, which did not undergo gradual deep burial, and the organic matter in the shale did not demonstrate the normal hydrocarbon generation process. The existence of a large amount of carbonized organic matter could clearly be observed via the scanning electron microscopy (Figure 5), indicating that the rapid thermal evolution cannot allow for rapid hydrogenation generation in the shale organic matter, and that complete hydrocarbon generation as well as the evolution of organic matter require a long process.

5.3. Shale Gas Exploration Prospect

The exploration prospect of shale gas is often closely associated with the evolution of organic matter, hydrocarbon generation, and the shale reservoir pore structure [20–28]. The Galedesi Formation shale in the Hala Lake Depression is a deep-water lacustrine deposit (Figure 3). Furthermore, a large amount of organic matter was enriched and retained in the Galedesi Formation shale during the deposition process. After the Indosinian orogeny, the frequent tectonic movement and magmatic thermal events in the South Qilian Basin rapidly baked the shale (Figure 8), and the organic matter in shale could not generate hydrocarbons through normal thermal evolution. Moreover, the gas content of the Galedesi Formation shale in the entire Hala Lake Depression was unusually low (Table 2). Therefore, from the perspective of the deposition, hydrocarbon generation, and reservoir, the shale gas exploration prospect of the Galedesi Formation in the study area is poor.

6. Conclusions

(1) The Galedesi Formation shale in the Hala Lake Depression of the South Qilian Basin is dominated by deep-lake facies, which has a large thickness, rich organic matter, and abnormally high thermal evolution. The diagenetic temperature of the shale was as high as 200 °C.

(2) After deposition, volcanic thermal events caused by multi-stage tectonic movements considerably affected the Galedesi Formation shale. High temperatures prevented the shale organic matter from generating hydrocarbons via the normal thermal evolution process; however, apparent carbonization occurred, indicating the possibility of continental shale gas exploration in this area.

Author Contributions: Data curation, C.Z. and X.G.; Funding acquisition, X.T.; Investigation, X.Q.; Methodology, L.L.; Resources, S.L. and L.X.; Software, N.J. and H.L.; Supervision, X.G.; Writing—review & editing, J.W. and X.T. All authors have read and agreed to the published version of the manuscript.

Funding: This research was funded by the National Natural Science Foundation of China, Grant Numbers 41902153 and 41672113, and the Natural Science Foundation Project of CQ CSTC, Grant Numbers cstc2018jcyjAX0523 and cstc2020jcyj-msxm0778.

Institutional Review Board Statement: Not applicable.

Informed Consent Statement: Not applicable.

Data Availability Statement: Not applicable.

Conflicts of Interest: The authors declare no conflict of interest.

References

1. Wenqing, W.; Chiyang, L.; Wenhui, L.; Xiaofeng, W.; Pei, G.; Jianqiang, W.; Zuodong, W.; Zhongping, L.; Dongdong, Z. Dominant products and reactions during organic matter radiolysis: Implications for hydrocarbon generation of uranium-rich shales. *Mar. Petrol. Geol.* **2022**, *137*, 105497. [CrossRef]
2. Bo, G.; Xiaoling, W.; Ying, Z.; Xinjun, C.; Ruikang, B.; Qianwen, L. Hydrocarbon generction and evolution characteristics of Triassic Zhangjiatan oil shale in southern Ordos Basin. *Pet. Geol. Exp.* **2022**, *44*, 24–32.
3. Xiugen, F.; Jian, W.; Wenbin, C.; Xinglei, F.; Dong, W.; Chunyan, S.; Shengqiang, Z. Elemental geochemistry of the early Jurassic black shales in the Qiangtang Basin, eastern Tethys: Constraints for palaeoenvironment conditions. *Geol. J.* **2016**, *51*, 443–454.
4. Caineng, Z.; Guosheng, Z.; Zhi, Y.; Shizhen, T.; Lianhua, H.; Rukai, Z.; Xuanjun, Y.; Qiquan, R.; Denghua, L.; Zhiping, W. Geological concepts, characteristics, resource potential and key techniques of unconventional hydrocarbon: On unconventional petroleum geology. *Pet. Explor. Dev.* **2013**, *40*, 385–399.
5. Wenzhi, Z.; Suyan, H.; Lianhua, H.; Tao, Y.; Xin, L. Types and resource potential of continental shale oil in China and its boundary with tight oil. *Pet. Explor. Dev.* **2020**, *47*, 1–11.
6. Jiamin, H.; Yue, Z.; Xiaowen, L.; Gang, X. Early Mesozoic deformations of the eastern Yanshan thrust belt, northern China. *Int. J. Earth Sci.* **2010**, *99*, 785–800.
7. Jinning, Z.; Jiansheng, Z.; Dunqing, X.; Guomeng, H.; Min, Z.; Lixin, F.; Hongjun, L.; Da, L. Control of the Mesozoic tectonic movement on the hydrocarbon generation and evolution of Upper Paleozoic coal-measure source rocks in the Huanghua Depression, Bohai Bay Basin. *Nat. Gas Ind.* **2019**, *39*, 1–10.
8. Sarkar, S.; Marfurt, K.J. Effect of volcanic bodies on hydrocarbon reservoirs in the northeastern part of the Chicontepec Foredeep, Mexico. *Interpret. J. Subsurf. Charact.* **2017**, *5*, SK1–SK10. [CrossRef]
9. Xixin, W.; Yuming, L.; Jiagen, H.; Shaohua, L. The relationship between synsedimentary fault activity and reservoir quality—A case study of the Ek1 formation in the Wang Guantun area, China. *Interpretation* **2020**, *8*, sm15–sm24. [CrossRef]
10. Xixin, W.; Xinrui, Z.; Shaohua, L.; Naidan, Z.; Ling, J.; Hang, L. Mechanism Study of Hydrocarbon Differential Distribution Controlled by the Activity of Growing Faults in Faulted Basins: Case Study of Paleogene in the Wang Guantun Area, Bohai Bay Basin, China. *Lithosphere* **2021**, 7115985.
11. Pasquarè, F.A.; Tormey, D.; Vezzoli, L.; Okrostsvaridze, A.; Tutberidze, B. Mitigating the consequences of extreme events on strategic facilities: Evaluation of volcanic and seismic risk affecting the Caspian oil and gas pipelines in the Republic of Georgia. *J. Environ. Manag.* **2011**, *92*, 1774–1782. [CrossRef] [PubMed]
12. Weihai, S.; Xinzhou, Z.; Pujun, W. Tertiary tectonic-volcanic events in the middle continental margin from eastern china and their control over oil-bearing basin. *J. Jilin Univ. Earth Sci. Ed.* **2003**, *33*, 479–484.
13. Xixin, W.; Fan, Z.; Shaohua, L.; Luxing, D.; Yuming, L.; Xiaoxu, R.; Depo, C.; Wen, Z. The Architectural Surfaces Characteristics of Sandy Braided River Reservoirs, Case Study in Gudong Oil Field, China. *Geofluids* **2021**, 8821711. [CrossRef]

14. Ancheng, X.; Long, Y.; Guangyao, X.; Junyong, Z.; Yongshu, Z.; Lei, W.; Haifeng, Z.; Suhua, Q. Triassic retroarc foreland basin in southern Qilian area: Evidence from sedimentary filling and tectonics. *Acta Petrol. Sin.* **2021**, *37*, 2385–2400. [CrossRef]
15. Haifeng, Y.; Jia, W.; Xianfeng, T.; Lei, C.; Cheng, Y.; Long, X.; Shiming, L.; Cong, J. Sedimentary characteristics of Permian-Triassic in Yangkang area, South Qilian Basin. *Pet. Geol. Exp.* **2019**, *41*, 699–716.
16. Yimeng, F. Investigatory summary of the Qilian Orogenic belt, China: History, presence and Prospect. *Adv. Earth Sci.* **1997**, *4*, 5–12.
17. Xiaoyuan, H.; Xinke, Y.; Yong, W.; Ruihua, G.; Zhaoyang, L.; Xianhu, W.; Shujuan, P. Geochemiacl and zircon U-Pb chronoligy of the volcanic rocks from the Balonggonggaer Formation in Tuergendaban, southern Qilian Mountain. *Acta Geol. Sin.* **2021**, *95*, 750–764.
18. Yongjiang, L.; Neubauer, F.; Weiming, L.; Genser, J.; Wei, L. Tectono-thermal events of the northern Qaidam margin-southern Qilian area, Western China. *J. Jilin Univ. Earth Sci. Ed.* **2012**, *42*, 1317–1329.
19. Qifeng, X.; Lifa, Z.; Yuanfeng, C.; Yu, L.; Zhiwu, L.; Suli, W. Geochmical characteristics of Permain marine source rocks and its constrains of the prcvenance and Paleoenvironment in the South Qilian Basin, Qinghai Province. *Acta Geol. Sin.* **2015**, *89*, 1288–1301.
20. Caineng, Z.; Songqi, P.; Qun, Z. On the connotation, challenge and significance of China's "energy independence" strategy. *Pet. Explor. Dev.* **2020**, *47*, 416–426.
21. Aisheng, H.; Jian, L.; Dongliang, W.; Zhisheng, L.; Junfeng, C.; Huiying, C.; Xiaohua, J. Biomarker characteristics of source rock of carboniferous and Upper Triassic Galedesi Formation in Southern Qilian Basin. *Unconv. Oil Gas* **2016**, *3*, 7–13.
22. Yu, T.; Genhou, W.; Yipeng, F.; Dan, C.; Dian, L.; Zhengze, F.; Xi, G.; Yufeng, W.; Jixin, H.; Peilie, Z. Tectonic-stratigraphic Properties and Evolution of the Yeba Volcanic Arc on the south of Gangdese, Tibet. *Earth Sci. Front.* **2022**, *29*, 285–302. [CrossRef]
23. Shijie, Z. Mantle dynamics on large spatial and temporal scales. *Chin. J. Geophys.* **2021**, *64*, 3478–3502.
24. Guoshuai, B.; Youlu, J.; Shuai, H.; Xingxia, C. Main controlling factors and genetic mechanism of high-quality volcanic reservoirs in the Huoshiling formation of the Longfengshan area. *Earth Sci.* **2021**. Available online: https://kns.cnki.net/kcms/detail/42.1874.P.20211025.1901.012.html (accessed on 12 May 2022).
25. Zengbao, H.; Jianping, Z.; Baohua, L.; Wei, Q.; Zhijun, W.; Xu, C. Age and Geochemistry of the Early Paleozoic Back-arc Type Ophiolite in Dadaoerji Area, South Qilian, China. *Geotecton. Metallog.* **2021**, *40*, 826–838.
26. Bo, J.; Jiyuan, Y.; Xiangming, L.; Botao, H.; Lei, W.L. The disintegration of Balonggongge'er Formation and the definition of lithostratigraphic unit in Danghenanshan area of South Qilian Mountain: Evidence from petrology and chronology. *Geol. Bull. China* **2018**, *37*, 621–633.
27. Xudong, B.; Bo, Y.; Zhongguo, Z.; Guangwen, O.Y.; Zhiqing, Z.; Chenglv, H. LA-MC-ICPMS zircon U-Pb dating and geochemical characteristics of Late Ordovician volcanic rocks in southern Qilian Mountains, Qinghai Provence. *Northwest. Geol.* **2018**, *51*, 125–136.
28. Ross, D.J.; Bustin, R. Characterizing the shale gas resource potential of Devonian-Mississippian strata in the Western Canada sedimentary basin: Application of an integrated formation evaluation. *AAPG Bull.* **2008**, *92*, 87–125. [CrossRef]
29. Dongfeng, H.; Zhihong, W.; Ruobing, L.; Xiangfeng, W.; Weiran, C.; Zhujiang, L. Enrichment control factors and exploration potential of lacustrine shale oil and gas: A case study of Jurassic in the Fuling area of the Sichuan Basin. *Nat. Gas Ind.* **2021**, *41*, 113–120.
30. Tonglou, G.; Yuping, L.; Zhihong, W. Reservoir-forming conditions of shale gas in Ziliujing Formation of Yuanba area in Sichuan Basin. *Nat. Gas Geosci.* **2011**, *22*, 1–7.
31. Xiangzeng, W.; Shengli, G.; Chao, G. Geological features of Mesozoic continental shale gas in south of Ordos Basin, NW China. *Pet. Explor. Dev.* **2014**, *41*, 294–304.
32. Jarvie, D. Unconventional shale resource plays: Shale gas shale oil opportunities. Tex. *Word Wide Geochem.* **2008**, 7–17. Available online: https://www.yumpu.com/en/document/view/10690125/unconventional-shale-resource-plays-shale-gas-and-shaleoil (accessed on 12 May 2022).
33. Ghareb, H.; Veronique, J. Developed correlations between sound wave velocity and porosity, permeability and mechanical properties of sandstone core samples. *Pet. Res.* **2020**, *5*, 326–338.